MATERIALS PHYSICS AND MECHANICS RESEARCH ARTICLE

Submitted: April 17, 2026 **Revised: May 8, 2026** **Accepted: June 2, 2026**

A refined model of thermoelastic energy dissipation in microbeam resonators

Ya.K. Astapov ✉, A.V. Lukin, I.A. Popov

Peter the Great St. Petersburg Polytechnic University, St. Petersburg, Russia

✉ astapov_yak@spbstu.ru

ABSTRACT

Thermoelastic damping is one of the main mechanisms of energy loss in nano- and microresonators. Thermoelastic damping assessment is traditionally explored for thermal boundary conditions of thermal insulation. In this work a classical Lifshitz-Roukes' model is extended to the case of a generalized Newton's law of cooling. Based on Bernoulli-Euler beam model, refined analytical expressions for complex eigenfrequencies and quality factor damping coefficient are derived. Taking into account heat flow in the longitudinal direction of the resonator. The results reveal that there are three qualitatively different cases, corresponding to thermal boundary conditions of thermal insulation, constant temperature and a mixture of both. Additionally, it is shown that the profile of each case significantly relies on geometric properties of the model.

KEYWORDS

MEMS • thermoelastic damping • Newton's law of cooling • heat transfer in solids

Funding. *The study was supported by the Russian Science Foundation grant No. 24-71-10097, https://rscf.ru/project/24-71-10097/.*

Citation: Astapov YaK, Lukin AV, Popov IA. A refined model of thermoelastic energy dissipation in microbeam resonators. *Materials Physics and Mechanics*. 2026;54(3): 54–63.
http://dx.doi.org/10.18149/MPM.5432026_5

Introduction

Nowadays, the nano- and microelectromechanical systems (N/MEMS) industry is undergoing rapid development. Sensors, actuators, energy and signal conversion systems based on N/MEMS technologies possess unique characteristics in terms of compactness, efficiency, and operational precision [1–5]. Often, the oscillating elements of N/MEMS are mechanical structures operating in a steady-state oscillation regime. The dynamic characteristics of such systems are significantly influenced by various mechanisms of vibrational energy dissipation.

Two types of energy dissipation mechanisms are distinguished: external and internal. External mechanisms include energy losses due to contact with gas or liquid media, anchor losses (wave energy leakage from the movable element to the device substrate through elastic suspensions), and surface losses [6]. Such losses can be minimized by selecting an appropriate geometry or by isolating the device from the environment [7–9], whereas internal mechanisms, such as thermoelastic dissipation or the presence of dopants in the material composition [6,10], are determined by the material properties. Consequently, they cannot be neutralized by external methods and will determine the upper limit of the system's quality factor. Thus, mathematical modeling of thermoelastic dissipation in the operational vibration modes of nano- and microresonators is an essential problem in the design of N/MEMS.

© Ya.K. Astapov, A.V. Lukin, I.A. Popov, 2026.
Publisher: Peter the Great St. Petersburg Polytechnic University
This is an open access article under the CC BY-NC 4.0 license (https://creativecommons.org/li-censes/by-nc/4.0/)

The study of two-way coupled dynamic problems of thermoelasticity has a long history [11]. The first work on thermoelastic dissipation for a beam of rectangular cross-section is generally considered to be that of C. Zener [12,13]. In his work, the author considers a viscoelastic material whose relaxation parameters determine the thermoelastic dissipation. Another work [14] examines a coupled thermoelastic problem formulated under the assumptions of the classical Bernoulli–Euler beam model combined with the heat equation. The authors successfully demonstrated good correlation with the results obtained by C. Zener, as well as revealed the presence of a damping extremum and investigated its dependence on the geometric parameters of the model. This theory was further developed in [15], where nonlocal continuum mechanics models were applied. In [16], the Timoshenko beam model was used instead of the Bernoulli–Euler beam. The authors provide comparisons of known models based on Zener's theory, the Bernoulli–Euler beam, and a finite element model. The work [17] reproduces the method developed by Lifshitz and Roukes for modeling thermoelastic energy dissipation in the flexural vibration modes of a thin ring.

In all the presented works, the description of the heat conduction process relies on Fourier's law. This approach corresponds to the assumption of an infinite speed of heat propagation in a body. One of the fundamental works dedicated to deriving and applying a modified heat conduction law that eliminates this paradox is the work of Lord and Shulman [18]. This work presents a heat propagation law that describes the acceleration of energy flow. Another approach consists of applying a modified Fourier law, which takes into account the first and subsequent time derivatives in the Taylor series expansion of the heat flux. Thus, the works [19,20] take into account one relaxation time component. The work [21] compares the classical models of Zener and Lifshitz–Roukes with the presented model, which accounts for two delay time components. The work [22] uses the approach proposed in [14] for a rotating annular resonator, taking into account two delay time components. The work [6] determines the system's damping considering three delay times. Works [23,24] present mathematical models of propagating waves in homogeneous isotropic and anisotropic thermoelastic media.

An original approach to solving the problem of increasing the quality factor of resonator oscillations is presented in the works [25,26]. The authors show that imparting a prestressed state to the system allows for an increase in the natural vibration frequencies and a reduction in the relaxation time, which leads to an improvement in the quality factor of the resonant properties. A comparison of several models accounting for body anisotropy is presented in [27].

In all the models presented, exclusively one type of thermal boundary condition on the free surface was considered, namely the thermal insulation condition. In the present work, we have developed the model proposed in [14] to the case of a generalized Newton’s law of cooling as the thermal boundary condition. To add, in mentioned works it is always assumed that heat flux occurs only laterally, but not longitudinally. In our work we take into account both directions.

Materials and Methods

We consider a bipinned thin beam of length *L*, width *b* and height *h*. The beam has a constant along its length rectangular cross-section and is made out of an isotropic homogeneous material. A stress-strain state of the model is fully described with its physical parameters, namely: mechanical – *Young's Modulus* (*E*), *Poisson's ratio* (*ν*), *density* (*ρ*); thermal – *conductivity coefficient* (k^T), *specific heat* (C^T), *coefficient of linear thermal expansion* (α^T).

The system of governing equations consists of coupled equation of motion and heat equation [14]:

$$\begin{cases} EI\frac{\partial^4 v}{\partial x^4} + \frac{\partial^2}{\partial x^2}\mathcal{M}^T + \rho A\frac{d^2 v}{dt^2} + E\alpha^T\frac{\partial^2 v}{\partial x^2}\int_A \theta\, dA = 0, \\ \frac{d\theta}{dt} = \kappa^T\frac{\partial^2}{\partial x^2}\theta + \kappa^T\frac{\partial^2}{\partial y^2}\theta - \frac{E\alpha^T T_0}{(1-2\nu)C^T\rho}\frac{d}{dt}\left[\varepsilon_x + \varepsilon_y + \varepsilon_z\right], \end{cases} \quad (1)$$

where $I = \int_A y^2\, dA = bh^3/12$ is a moment of inertia, $\mathcal{M}^T = E\alpha^T\int_A y\theta\, dA$ is a thermal bending moment, $\kappa^T = k^T/(C^T\rho)$ is a thermal diffusivity, $\left.\begin{aligned} \varepsilon_x &= -y\frac{\partial^2 v}{\partial x^2} \\ \varepsilon_y = \varepsilon_z &= \nu y\frac{\partial^2 v}{\partial x^2} + (1+\nu)\alpha^T\theta \end{aligned}\right\}$ are diagonal components of the strain tensor according to the Euler-Bernoulli beam model, $\theta(x,y,t) = T(x,y,t) - T_0$ is a relative temperature.

Then we define non-dimensional parameters:

$$\begin{aligned} x = \check{x}L, \quad y = \check{y}h, \quad z = \check{z}b, \quad t = \frac{1}{\omega_0}\tau, \\ v = \check{v}L, \quad \theta = \check{\theta}T_0, \end{aligned} \quad (2)$$

so that Eq. (1) becomes:

$$\begin{cases} \frac{\partial^4\check{v}}{\partial\check{x}^4} + \frac{\check{\alpha}^T\delta}{\check{I}}\frac{\partial^2}{\partial\check{x}^2}\int_{-\frac{1}{2}}^{\frac{1}{2}}\check{y}\check{\theta}\, d\check{y} + \frac{d^2\check{v}}{d\tau^2} + \frac{\check{\alpha}^T\delta^2}{\check{I}}\frac{\partial^2\check{v}}{\partial\check{x}^2}\int_{-\frac{1}{2}}^{\frac{1}{2}}\check{\theta}\, d\check{y} = 0, \\ \hat{p}\frac{d\check{\theta}}{d\tau} = \check{\kappa}^T\frac{\partial^2\check{\theta}}{\partial\check{x}^2} + \check{\kappa}^T\delta^2\frac{\partial^2\check{\theta}}{\partial\check{y}^2} + \frac{\Delta_E}{\check{\alpha}^T}\frac{1}{\delta}\check{y}\frac{d}{d\tau}\frac{\partial^2\check{v}}{\partial\check{x}^2}, \end{cases} \quad (3)$$

where $\omega_0 = \sqrt{EI/(\rho AL^4)}$ is a relative radial frequency, $\check{\alpha}^T = \alpha^T T_0$ is a non-dimensional coefficient of linear thermal expansion, $\check{I} = I/bh^3$ is a non-dimensional moment of inertia, $\check{\kappa}^T = \kappa^T/(L^2\omega_0)$ is a non-dimensional thermal diffusivity, $\delta = L/h$ is a non-dimensional geometric parameter, $\Delta_E = E{\alpha^T}^2T_0/(C^T\rho)$ is a relaxation strength, $\hat{p} = 1 + 2\Delta_E(1+\nu)/(1-2\nu)$.

The first term of the right-hand side of the heat equation in Eq. (3) corresponds to heat flux in a longitudinal direction that is usually neglected, as it is considered that heat flux in lateral direction prevails. However, in the cases of thick beams ($\delta \to 1$) it has an impact on the results and should not be neglected.

Solution of Eq. (3) can be searched for in a form:

$$\check{v}(\check{x},\tau) = \sum_{n=1}^{\infty}\phi_n\sin(\pi n\check{x})\, e^{i\check{\omega}\tau}, \quad \check{\theta}(\check{x},\check{y},\tau) = \sum_{n=1}^{\infty}F_n(\check{y})\sin(\pi n\check{x})\, e^{i\check{\omega}\tau}. \quad (4)$$

Substituting Eq. (4) into Eq. (3) and applying the orthogonality condition yields a system of differential equations of *j*-modes:

$$\frac{\partial^2 F_j}{\partial\check{y}^2} - \underbrace{\frac{1}{\delta^2}\left(\pi^2j^2 + i\frac{\hat{p}\check{\omega}}{\check{\kappa}^T}\right)}_{\lambda_j^2}F_j - i\check{\omega}\pi^2j^2\frac{\Delta_E}{\check{\kappa}^T\check{\alpha}^T}\frac{1}{\delta^3}\check{y} = 0 \quad (j = 1,2,3,\dots,)$$

Exact solution has a form:

$$F_j = D_1 e^{\lambda_j \breve{y}} + D_2 e^{-\lambda_j \breve{y}} - i\pi^2 j^2 \frac{\breve{\omega}}{\lambda_j^2} \frac{\Delta_E}{\breve{\kappa}^T \breve{\alpha}^T} \frac{\phi_j}{\delta^3} \breve{y}, \quad (j = 1,2,3,\dots,) \tag{5}$$

where D_1, D_2 are unknown integration coefficients which are to be found from thermal boundary conditions.

Thermal boundary conditions are applied to free surfaces of the model ($\breve{y} = \pm 1/2$) and are defined in a general form according to Newton's law of cooling:

$$\left[\pm k^T \frac{\partial \theta}{\partial y} + h^T \theta\right]\Big|_{y=\pm\frac{h}{2}} = 0, \tag{6,a}$$

where h^T is a coefficient of heat transfer. In non-dimensional terms the law has a form:

$$\left[\pm \frac{\partial \breve{\theta}}{\partial \breve{y}} + \breve{\mu}^T \breve{\theta}\right]\Big|_{\breve{y}=\pm\frac{1}{2}} = 0, \tag{6,b}$$

where $\breve{\mu}^T = h^T h / k^T$.

Substituting Eq. (5) into Eq. (6,b) yields an expression for the temperature field:

$$\breve{\theta}(\breve{x}, \breve{y}, \tau) = \sum_{n=1}^{\infty} \left[-i \frac{\breve{\omega} \phi_n \pi^2 n^2 \Delta_E}{\lambda_n^2 \breve{\kappa}^T \breve{\alpha}^T \delta^3} \left(\breve{y} - \widehat{D}_n \sinh(\lambda_n \breve{y})\right) \sin(\pi n \breve{x})\, e^{i\breve{\omega}\tau}\right], \tag{7}$$

where $\widehat{D}_n = \frac{(1+\breve{\mu}^T/2)}{\left[\lambda_n \cosh\left(\frac{\lambda_n}{2}\right) + \breve{\mu}^T \sinh\left(\frac{\lambda_n}{2}\right)\right]}$.

We can now use Eq. (7) to receive a transcendental equation for eigenfrequency by applying Eqs. (4) and (7) to the first equation in the system (3):

$$\sum_{n=1}^{\infty} \pi^4 n^4 \phi_n \sin(\pi n \breve{x})\, e^{i\breve{\omega}\tau} +$$
$$+ \frac{\breve{\alpha}^T \delta}{\breve{I}} \sum_{n=1}^{\infty} \left[\frac{i\pi^4 n^4 \breve{\omega} \Delta_E \phi_n}{\lambda_n^2 \breve{\kappa}^T \breve{\alpha}^T \delta^3} \int_{-\frac{1}{2}}^{\frac{1}{2}} \left(\breve{y}^2 - \widehat{D}_n \breve{y} \sinh(\lambda_n \breve{y})\right) d\breve{y}\right] \sin(\pi n \breve{x})\, e^{i\breve{\omega}\tau} -$$
$$- \breve{\omega}^2 \sum_{n=1}^{\infty} \phi_n \sin(\pi n \breve{x})\, e^{i\breve{\omega}\tau} + \frac{\breve{\alpha}^T \delta^2}{\breve{I}} \sum_{m=1}^{\infty} \left[\pi^2 n^2 \phi_m \sin(\pi m \breve{x})\, e^{i\breve{\omega}\tau}\right] \cdot$$
$$\cdot \sum_{n=1}^{\infty} \left[\frac{i\breve{\omega}\pi^2 n^2 \Delta_E \phi_n}{\lambda_n^2 \breve{\kappa}^T \breve{\alpha}^T \delta^3} \int_{-\frac{1}{2}}^{\frac{1}{2}} \left(\breve{y} - \widehat{D}_n \sinh(\lambda_n \breve{y})\right) d\breve{y}\right] \sin(\pi n \breve{x})\, e^{i\breve{\omega}\tau} = 0.$$

As it can be seen, the equation above is nonlinear with respect to the coefficients ϕ_n as the last part of the equation contains $\sum_n \sum_m \phi_n \phi_m$. Further, we will neglect this term as it brings a small perturbation in a total solution. Thus, by applying an orthogonality condition, a transcendental equation for an eigenfrequency of j^{th} form is deduced:

$$\breve{\omega}_j^2 = \pi^4 j^4 \left\{1 + \frac{i\breve{\omega}_j \Delta_E}{\lambda_j^2 \breve{\kappa}^T \delta^2} \left[1 - \frac{\widehat{D}_j}{\breve{I}} \left(\frac{\cosh\left(\frac{\lambda_j}{2}\right)}{\lambda_j} - \frac{2\sinh\left(\frac{\lambda_j}{2}\right)}{\lambda_j^2}\right)\right]\right\}, \quad (j = 1,2,3,\dots,) \tag{8,a}$$

where $\lambda_j = \frac{1}{\delta}\sqrt{\pi^2 j^2 + i\breve{\omega}_j \frac{\hat{p}}{\breve{\kappa}^T}}$, $\widehat{D}_j = \frac{(1+\breve{\mu}^T/2)}{\left[\lambda_j \cosh\left(\frac{\lambda_j}{2}\right) + \breve{\mu}^T \sinh\left(\frac{\lambda_j}{2}\right)\right]}$.

We rewrite Eq. (8,a) in a more compact form:

$$\breve{\omega}_j^2 = \pi^4 j^4 \{1 + H_j(\breve{\omega}_j)\}, \qquad (j = 1,2,3,\dots,) \tag{8,b}$$

where $H_j(\breve{\omega}_j) = i \frac{\breve{\omega}_j}{\lambda_j^2} \frac{\Delta_E}{\breve{\kappa}^T \delta^2} \left[1 - \frac{\widehat{D}_j}{\breve{I}} \left(\frac{\cosh\left(\frac{\lambda_j}{2}\right)}{\lambda_j} - \frac{2\sinh\left(\frac{\lambda_j}{2}\right)}{\lambda_j^2}\right)\right]$.

It can be seen that Eq. (8,b) is similar with a case of a purely elastic bipinned beam oscillating when there is no thermal expansion observed $\breve{\alpha}^T = \Delta_E = 0$. A term $H_j(\breve{\omega}_j)$ is a small complex additive that takes into consideration a thermo-elastic coupling. Since Eq. (8,b) is transcendental, the solution is found via numerical or asymptotic methods.

We apply the perturbation method to Eq. (8,b) [28]. Since $H_j(\breve{\omega}_j)$ is small we rewrite Eq. (8,b) in a more sufficient form by introducing a small parameter ϵ:

$$\breve{\omega}_j^2 = \pi^4 j^4\{1 + H_j(\breve{\omega}_j)\} \quad \rightarrow \quad \breve{\omega}_j^2 = \pi^4 j^4\{1 + \epsilon G_j(\breve{\omega}_j)\}. \tag{9}$$

An approximate solution has a form:

$$\breve{\omega}_j \approx \breve{\omega}_j^* + \epsilon\sigma_1 + \epsilon^2\sigma_2 + \cdots, \tag{10}$$

where $\breve{\omega}_j^* = \pi^2 j^2$ is an exact solution of a purely elastic case, $\sigma_1, \sigma_2, \ldots$ are unknown additives.

We expand the transcendental part $G_j(\breve{\omega}_j)$ in (9) in Taylor series around $\epsilon = \epsilon^* = 0$:

$$G_j\left(\breve{\omega}_j^* + \epsilon\sigma_1 + O(\epsilon^2)\right) \approx \sum_{r=0}^{\infty} \frac{G_j^{(r)}\big|_{\epsilon=\epsilon^*}}{r!}(\epsilon - \epsilon^*)^r. \tag{11}$$

Substituting Eqs. (10) and (11) into Eq. (9) and taking into consideration only terms with ϵ^1 yields an expression for the first additive:

$$\sigma_1 = \frac{\breve{\omega}_j^* G_j(\breve{\omega}_j^*)}{2}. \tag{12}$$

And thus $\breve{\omega}_j \approx \breve{\omega}_j^* + \epsilon\frac{\breve{\omega}_j^* G(\breve{\omega}_j^*)}{2}$.

Due to the fact that ϵ is a bool-keeping parameter, we assume it to be $\epsilon = 1$, so that the final solution is:

$$\breve{\omega}_j \approx \breve{\omega}_j^* + \frac{\breve{\omega}_j^* G(\breve{\omega}_j^*)}{2}, \qquad (j = 1,2,3,\ldots), \tag{13}$$

where $G_j(\breve{\omega}_j^*) = H_j(\breve{\omega}_j^*) = i\frac{\breve{\omega}_j^*}{\lambda_j^{*2}}\frac{\Delta_E}{\breve{\kappa}^T\delta^2}\left[1 - \frac{\widehat{D}_j^*}{I}\left(\frac{\cosh\left(\frac{\lambda_j^*}{2}\right)}{\lambda_j^*} - \frac{2\sinh\left(\frac{\lambda_j^*}{2}\right)}{\lambda_j^{*2}}\right)\right]$,

$\widehat{D}_j^* = \frac{\left(1+\breve{\mu}^T/2\right)}{\left[\lambda_j^*\cosh\left(\frac{\lambda_j^*}{2}\right)+\breve{\mu}^T\sinh\left(\frac{\lambda_j^*}{2}\right)\right]}$, $\lambda_j^* = \frac{1}{\delta}\sqrt{\breve{\omega}_j^*\left(1 + i\frac{\hat{p}}{\breve{\kappa}^T}\right)}$.

Having received model's eigenfrequencies, we may assess the dissipation coefficient of the model Q^{-1} for the case of small attenuation with

$$Q^{-1} = 2\left|\frac{\mathrm{Im}\{\breve{\omega}\}}{\mathrm{Re}\{\breve{\omega}\}}\right|, \tag{14}$$

where Q is the quality factor of the considered eigenmode of the resonator.

Results

Two materials: monocrystalline Silicon and α-quartz (SiO_2) – are often used in the manufacturing of high-quality resonators. Here, the materials are considered isotropic. Their physical properties are listed in Table 1. Geometric properties of the microbeam are listed in Table 2.

Table 1. Physical properties of materials

Name	**Units**	**Si**	**SiO_2**
Mechanical properties			
E	[GPa]	160	68
ν	[–]	0.27	0.17
ρ	[kg/m^3]	2330	2225
Thermal properties			
α^T	[1/K]	$2.6\cdot10^{-6}$	$0.6\cdot10^{-6}$
k^T	[W/(m·K)]	130	1.38
C^T	[J/(kg·K)]	700	1000

Table 2. Geometric properties of the beam

L, μm	500	h, μm	40	b, μm	100

An impact of variation of physical and geometric properties of the model, namely heat transfer coefficient h^T and height h, respectively, on the damping coefficient of the model for Si and SiO_2 is shown in Fig. 1. As it can be seen, numerical and asymptotical approaches, defined with Eqs. (8) and (13), respectively, give nearly equal solutions. Figures 1(a,c) illustrate that by varying geometric properties of the model, one may find the maximum value of dissipation. It is noticeable that maximums occur at different

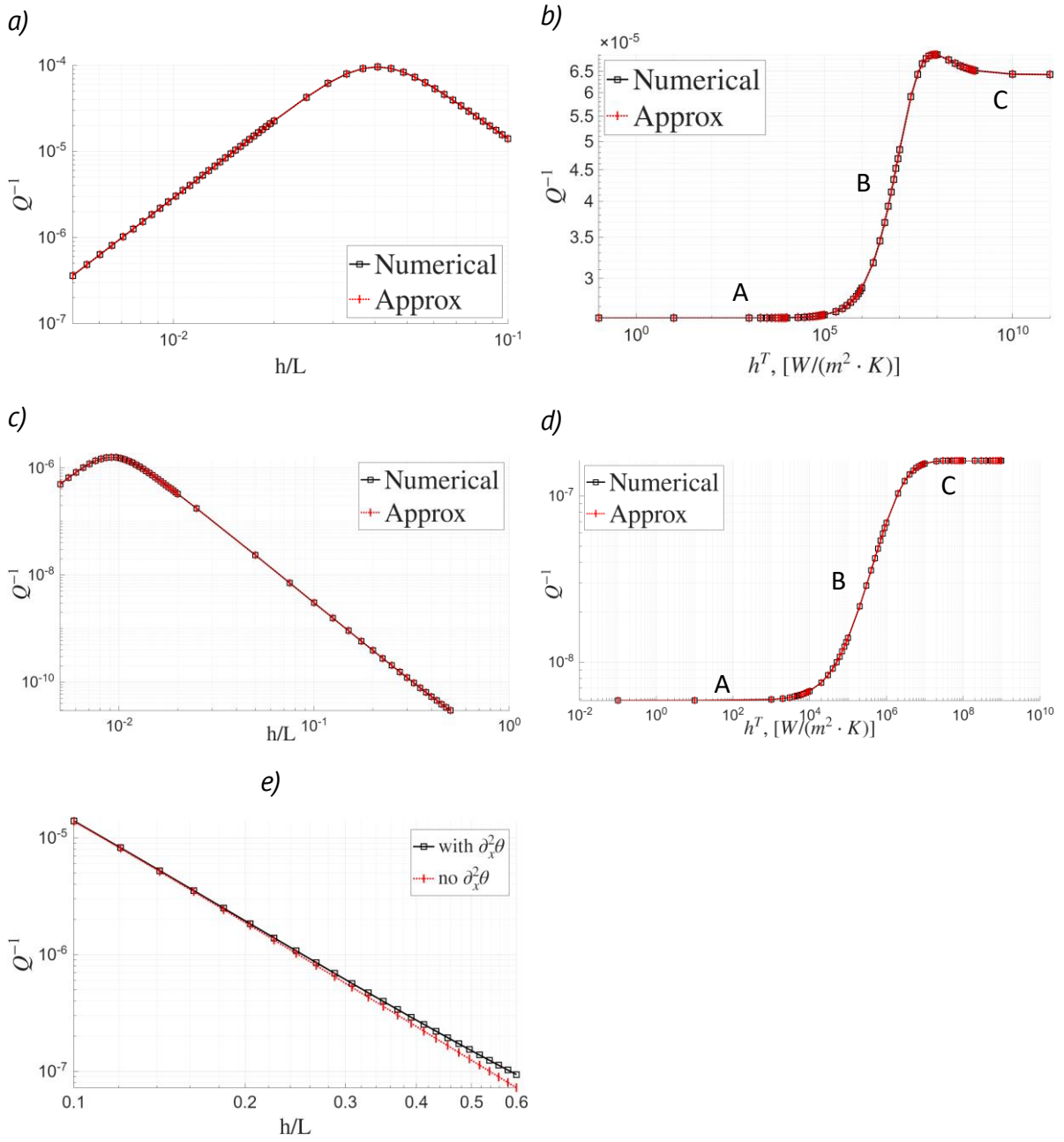


Fig. 1. An impact of geometrical, namely relative height (a,c), and physical – heat transfer coefficient (b,d) – properties on damping coefficient of the beam, made out of Si (a,b) and SiO_2 (c,d); (e) an impact of longitudinal heat flux presence on damping coefficient for Si

relative heights: $h/L \approx 0.04$ for Si and $h/L \approx 0.01$ for SiO_2. It is also remarkable that the damping in SiO_2 is 2 orders of magnitude smaller than in Si. Figures 1(b,d) show an impact of the interaction between the model and the surrounding space, defined with the heat transfer coefficient, on the dissipation. We distinguish three graph areas that correspond to different cases: area A corresponds to the case of thermal insulation when there is no heat flux on the free surface occurring and, hence, temperature of beam's surface is not affected by the environment temperature; area B corresponds to the mixed case when there is small amount of heat flux happening and the surface temperate is slightly affected by the temperature around; area C corresponds to the case when all heat radiates from the surface into environment, what means that the surface temperature is always equal to the temperature of the adjoin space. Areas A and C have constant values of the damping coefficient. The drop of dissipation from area C to area A is 3 times for Si, and is about two orders of magnitude for SiO_2. Area B represents a rapid transfer from case A to case C. In the case of Si area B begins at $h^T \approx 10^5$ W/m^{2}K, while in the case of SiO_2 it begins at $h^T \approx 10^3$ W/m^{2}K. Usually, resonating systems have the value of the heat transfer coefficient in area A ($h^T \in [1, 10^2]$) meaning a negligibly small thermal interaction between the model and the surrounding space. However, it was shown [29,30] that the heat transfer coefficient may have the value up to 10^6 for micro- and nano- beams. Such values correspond to area B and, as it can be seen from the figures, it may have a significant effect on the dissipation in the system. To add, in Fig. 1(b) area B has an extremum and in Fig. 1(d) there is no such. The reason for an emergence of extremum value is due to geometric properties of the beam as it will be shown further. Figure 1(e) illustrates an impact of longitudinal heat flux presence in (1) and (3) on the quality factor of the microbeam. It is seen that, indeed, for thick beams an impact is noticeable.

Figure 2 shows the damping coefficient for different values of physical and geometrical properties. As it can be seen, changing the value of the heat transfer coefficient shifts the maximum value of dissipation. On the other hand, varying the relative height changes the profile of $h^T - Q^{-1}$ dependency. For thin beams ($h/L \sim 0.01$ for Si, and $h/L \sim 0.001$ for SiO_2), dissipation in the case of thermal insulation (area A) is higher than in the case of constant temperature (area C). But for thick beams ($h/L \sim 0.15$ for Si, and $h/L \sim 0.5$ for SiO_2) dissipation at area A is lower than at area C, which means that the height of the beam plays a significant role on the amount of dissipation occurring in each case. Moreover, there is a specific area of relative height values ($h/L \sim 0.06$ for Si, and $h/L \sim 0.013$ for SiO_2) when the $h^T - Q^{-1}$ profile obtains a local extremum, shown in Fig. 1(c). In other cases, the profile has no local extremums.

In Fig. 3(a), one time-period oscillations of temperature distribution along the beam's height at $\breve{x} = 1/2$ for both materials at different thermal cases are shown. Colours represent areas of heating (yellow) and freezing (blue). As it can be seen from Fig. 1(a,d) that corresponds to the case of thermal insulation, local thermal extremums occur on free surfaces of the beam and there is no interaction between the model and the surrounding area occurring. As the value of the heat transfer coefficient increases, those local extremums "sinks" into depth of the beam. In Fig. 3(c,f) that correspond to the last case, the temperature at the free surfaces is constant and equals to the temperature of the surrounding area. It is also noticeable that the depth, local extremums sink into, differs for Si and SiO_2.

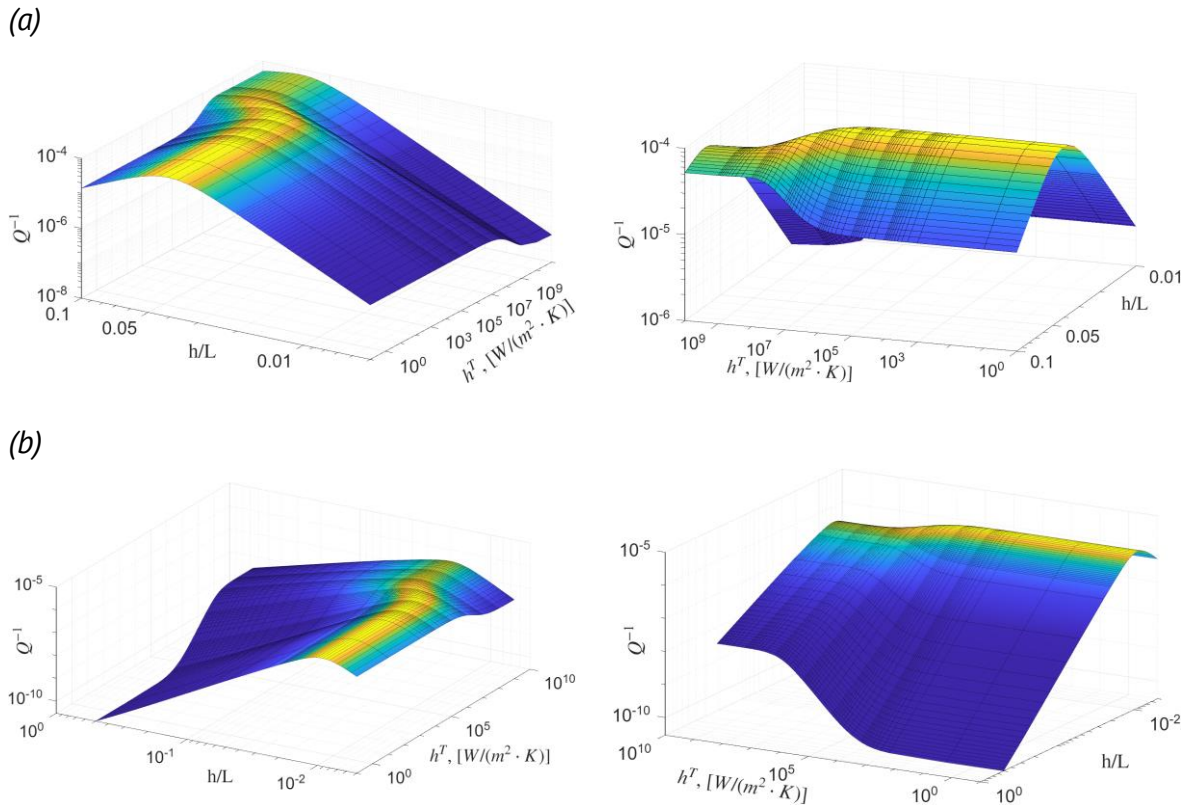


Fig. 2. Damping coefficient for different geometric and physical properties for (a) Si; (b) SiO_2 (different viewing angles)

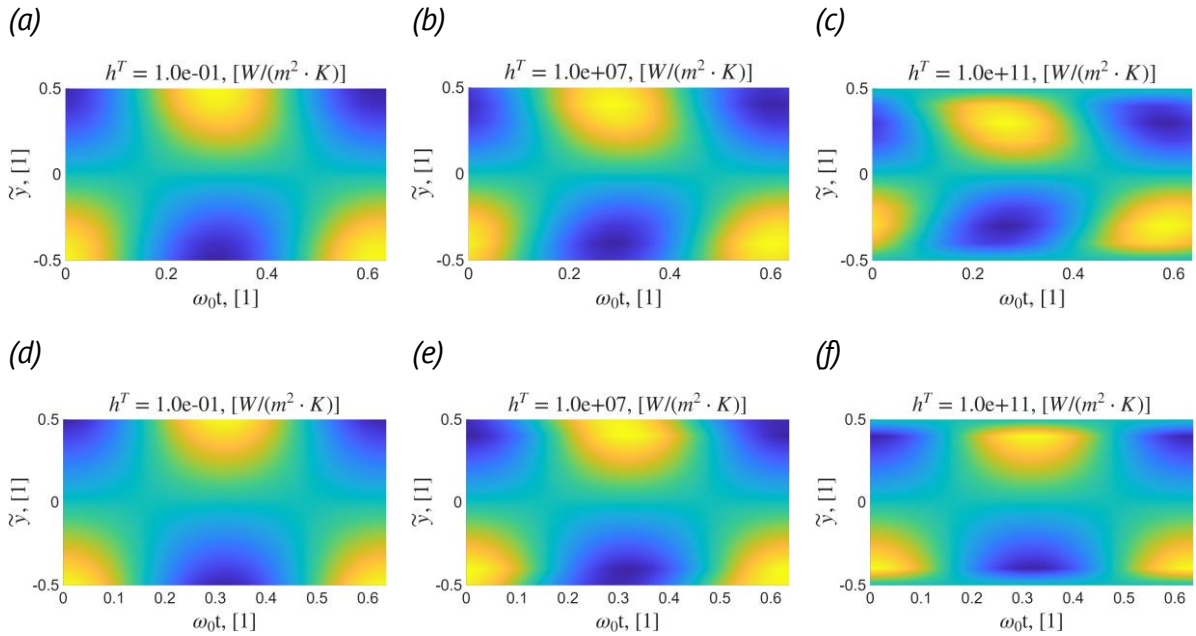


Fig. 3. Oscillations of temperature distribution along beam's height at $\tilde{x} = 1/2$ for one time period for Si (a,b,c) and SiO_2 (d,e,f). Figures (a) and (d) correspond to the case of thermal insulation; figures b) and e) correspond to mixed case; and figures (c) and (f) correspond to the case of constant temperature

Conclusions

This paper presents results of analytical derivation of the mathematical model of a bipinned beam in thermoelastic domain. Heat flux in both longitudinal and lateral directions is regarded. An impact of thermal interaction between the beam and adjoining space on energy dissipation is shown. Thermal boundary conditions are defined by a generalized Newton's law of cooling. A perturbation approach for solving the transcendental equation is discussed. It is shown that the asymptotic approach has very good accuracy. The results are presented for Si and SiO_2, which are commonly used in the manufacturing of resonators.

Three qualitatively different cases are observed at the beam's free surfaces: thermal insulation, constant temperature and a mixed case. It is shown that for nano- and micro-beams the impact of thermal interaction may be significant and cannot be neglected. Moreover, the profile of each case is crucially affected by the geometric properties of the model.

CRediT authorship contribution statement

Yaroslav K. Astapov: writing – review & editing, writing – original draft, investigation; **Alexey V. Lukin**: writing – review & editing, conceptualization, supervision; **Ivan A. Popov**: supervision

Conflict of interest

The authors declare that they have no conflict of interest.

References

1. Ekinci KL, Roukes ML. Nanoelectromechanical systems. *Review of Scientific Instruments.* 2005;76(6): 061101.
2. Komarevtsev IM, Kondrateva AS, Kazakin AN, Enns YaB, Lazdin IA, Karaseov PA, Akulshin UD. Microelectromechanical gas sensor of resistive type for detection of hydrogen sulfide down to low concentrations. *Materials Physics and Mechanics.* 2024;52(4): 9–22.
3. Cheng J, Xue N, Qiu B, Zhao Q, Gang F, Yao Z, Zhou W, Sun X. Recent Design and Application Advances in Micro-Electro-Mechanical System (MEMS) Electromagnetic Actuators. *Micromachines.* 2025;16(6): 670.
4. Shen Y. Current Status and Application of Micro-electromechanical Systems (MEMS). *Engineering and Technology.* 2023;46: 97–105.
5. Lu S, Shen Y, Hou F, Wan F, Ding Y, Lin Z, Hu S. Silicon-based MEMS hybrid packaging approach for tetrahertz front-end integration: architecture, design, and prototype validation. *Science China Information Sciences.* 2026;69: 150303.
6. Kumar R, Kumar R, Kumar H. Effects of phase-lag on thermoelastic damping in micromechanical resonators. *Thermal Stresses.* 2018;41(9): 1115–1124.
7. Nguyen CC, Li WL. Influences of temperature on the quality factors of micro-beam resonators in gas rarefaction. *Sensors and Actuators A: Physical.* 2017;261: 151–165.
8. Fang D, Sun Y, Soh AK. Advances in Thermoelastic Damping in Micro- and Nano- Mechanical Resonators: a Review. *Solid Mechanics and Materials Engineering.* 2007;1(1): 18–34.
9. Kazemi M, Nabavi S, Gratuze M, Nabki F. Anchor Loss Reduction in Micro-Electro Mechanical Systems Flexural Beam Resonators Using Trench Hole Array Reflectors. *Micromechanics.* 2023;14(11): 2036.
10. Serdean F, Pustan M, Dudescu C, Birleanu C, Serdean M. Analysis of the Thermoelastic Damping Effect in Electrostatically Actuated MEMS Resonators. *Mathematics.* 2020;8(7): 1124.
11. Landau LD, Lifshitz EM. *Theory of Elasticity. Vol. 7.* 3rd ed. Butterworth-Heinemann; 1986.

12. Zener C. Internal Friction in Solids. I. Theory of Internal Friction in Reeds. *Physical Review.* 1937;52: 230–235.
13. Zener C. Internal Friction in Solids II. General Theory of Thermoelastic Internal Friction. *Physical Review.* 1938;53(1): 90–99.
14. Lifshitz R, Roukes M. Thermoelastic damping in micro- and nanomechanical systems. *Physical Review.* 2000;61(8): 5600–5609.
15. Yu YJ, Tian XG, Liu J. Size-dependent damping of a nanobeam using nonlocal thermoelasticity extension of Zener, Lifshitz, and Roukes' damping model. *Acta Mechanica.* 2017;228: 1287–1302.
16. Parayil DV, Kulkarni SS, Pawaskar DN. Analytical and numerical solutions for thick beams with thermoelastic damping. *International Journal of Mechanical Sciences.* 2015;94–95: 10–19.
17. Wong SJ, Fox CHJ, McWilliam S. Thermoelastic damping of the in-plane vibration. *Sound and Vibration.* 2006;293: 266–285.
18. Lord HW, Shulman Y. A generalized dynamical theory of thermoelasticity. *J. Mech. Phys. Solids.* 1967;15: 299–309.
19. Sun Y, Fang D, Soh AK. Thermoelastic damping in micro-beam resonators. *International Journal of Solids and Structures.* 2006;43(10): 3213–3229.
20. Kumar R, Singhal P. Temperature-dependent phase leg and non-local thermoelastic damping and frequency shift in thermoelastic plates. *Materials Physics and Mechanics.* 2025;53(3): 94–115.
21. Guo FL, Wang GQ, Rogerson GA. Analysis of thermoelastic damping in micro- and nanomechanical resonators based on dual-phase-lagging generalized thermoelasticity theory. *International Journal of Engineering Science.* 2012;60: 59–65.
22. Alghamdi NA, Youssef HM. Dual-phase-lagging thermoelastic damping in-extensional vibration of rotating nano-ring. *Microsystem Technologies.* 2017;23: 4333–4343.
23. Kumar R, Sharma P. Some theorrems and wave propagation in a piezothermoelastic medium with two-temperature and fractional order derivative. *Materials Physics and Mechanics.* 2021;47(2): 196–218.
24. Kaushal S, Kumar R, Bala I, Sharma G. Impact of non-local, two temperature and impedance parameters on propagation of waves in generalized thermoelastic medium under modified Green-Lindsay model. *Materials Physics and Mechanics.* 2024;52(1): 1–17.
25. Kumar S, Haque A. Stress-dependent thermal relaxation effects in micro-mechanical resonators. *Acta Mechanica.* 2010;212: 83–91.
26. Kumar S, Haque A, Alam T. Thermo-mechanical coupling and size effects in micro and nano resonators. *Micro and Nano Systems Letters.* 2013;1: 1–9.
27. Sharma JN, Sharma R. Damping in micro-scale generalized thermoelastic circular plate resonators. *Ultrasonics.* 2011;51: 352–358.
28. Nayfeh AH. *Perturbation Methods*. WILEY-VCH Verlag GmbH & Co. KGaA, Weinheim; 2004.
29. Fu CJ, Zhang ZM. Nanoscale radiation heat transfer for silicon at different doping levels. *International Journal of Heat and Mass Transfer.* 2006;49(9–10): 1703–1718.
30. Benther JD, Pelaez-Restrepo JD, Stanley C, Rasengarten G. Heat transfer during multiple droplet impingement and spray cooling: Review and prospects for enhanced surfaces. *International Journal of Heat and Mass Transfer.* 2021;178: 121587.